THE JOURNAL OF BIOLOGICAL CHEMISTRY VOL. 282, NO. 9, pp. 6525–6531, March 2, 2007

Structural Mechanism and Photoprotective Function of Water-soluble Chlorophyll-binding Protein*

Received for publication, October 6, 2006, and in revised form, December 14, 2006 Published, JBC Papers in Press, December 14, 2006, DOI 10.1074/jbc.M609458200

Daisuke Horigome[‡§1], Hiroyuki Satoh[‡], Nobue Itoh[¶], Katsuyoshi Mitsunaga[‖], Isao Oonishi[‡], Atsushi Nakagawa[§2], and Akira Uchida[‡2,3]

From the [‡]Department of Biomolecular Science, [¶]Faculty of Science, Toho University, 2-2-1 Miyama, Funabashi, Chiba 274-8510, Japan, the [‖]School of Pharmaceutical Sciences, Toho University, 2-2-1 Miyama, Funabashi, Chiba 274-8510, Japan, and the [§]Institute for Protein Research, Osaka University, 3-2 Yamadaoka, Suita, Osaka 565-0871, Japan

A water-soluble chlorophyll-binding protein (WSCP) is the single known instance of a putative chlorophyll (Chl) carrier in green plants. Recently the photoprotective function of WSCP has been demonstrated by EPR measurements; the light-induced singlet-oxygen formation of Chl in the WSCP tetramer is about four times lower than that of unbound Chl. This paper describes the crystal structure of the WSCP-Chl complex purified from leaves of *Lepidium virginicum* (Virginia pepperweed) to clarify the mechanism of its photoprotective function. The WSCP-Chl complex is a homotetramer comprising four protein chains of 180 amino acids and four Chl molecules. At the center of the complex one hydrophobic cavity is formed in which all of the four Chl molecules are tightly packed and isolated from bulk solvent. With reference to the novel Chl-binding mode, we propose that the photoprotection mechanism may be based on the inhibition of physical contact between the Chl molecules and molecular oxygen.

Water-soluble chlorophyll-binding proteins (WSCPs),[4] which form a complex with chlorophyll (Chl), have been isolated from Amaranthaceae, Chenopodiaceae, and Polygonaceae (class-I) and from Brassicaceae (class-II). The two WSCP classes differ in that the protein-Chl complexes of the former change their absorption spectra upon illumination, whereas those of the latter show no photoconversion of their absorption behavior (2). The amino acid sequence of class-I WSCP shows no similarity to that of class-II WSCP.

The class-II WSCPs (hereafter referred to as "WSCPs") are water-soluble proteins of ~20 kDa, which form a tetrameric assembly upon binding Chl molecules with a Chl-to-protein ratio of one or less, and exhibit high thermal and photostability (1, 3). The physiological function of WSCPs is still not known. Although WSCPs have a sequence similarity of ~30% with Künitz-type proteinase inhibitors, no significant protease inhibitor activity of WSCPs has yet been identified (4–6). The low Chl content per protein makes it unlikely that WSCPs are involved in the light reaction of photosynthesis. Meanwhile, it has been speculated (7, 8) that WSCP acts as a scavenger of free Chl, by transporting it from the thylakoid membrane to the chloroplast envelope, where Chlase, the enzyme that initiates the Chl catabolism, is thought to reside (9).

An *in vitro* binding assay with the recombinant apo-WSCP cloned from cauliflower (*Brassica oleralcea* var. Botrys) and Chl or its derivatives showed that the central Mg^{2+} ion and the phytyl tail of Chl were essential for protein-pigment binding and tetrameric assembly, respectively (1). Furthermore, the recombinant apo-WSCP was able to remove Chl from the thylakoid membrane *in vitro* and organize the tetrameric WSCP-Chl complex (3). The absorption spectrum of the reconstituted complex is very similar to that of the native WSCP-Chl complex purified from fresh leaves (1, 3).

The WSCP-Chl complex retains its fresh green color under dim light for months, enough for a long term crystallization experiment. Free Chl, on the other hand, shows color fading within a day due to unavoidable photooxidation in the presence of molecular oxygen under visible light irradiation. Absorption of light quanta by Chl initially results in excitation to a singlet state (^{1}Chl). If the energy is not efficiently used through photosynthetic electron transport, the triplet (^{3}Chl) state follows, which upon contact with molecular oxygen generates the singlet oxygen species. Photodynamic damage including the oxidative decomposition of Chl itself can be propagated by the singlet oxygen species, giving rise to radical oxygen species *in vivo* as well as *in vitro* (10, 11). The risk of radical oxygen species generation in the thylakoid membrane is usually diminished by non-photochemical quenching by carotenoids, which are adjacent to Chl molecules in virtually all Chl-containing complexes and quench both the ^{3}Chl and the singlet oxygen (12, 13). In view of this, one would expect that the WSCP-Chl complex also contains carotenoids to avoid the risk of radical oxygen species generation. However, no carotenoids have been found in native WSCPs, and EPR measurements using the reconstituted

* This work was supported in part by a grant-in-aid for the 21st Century Centers of Excellence (COE) program and by the National Project on Protein Structural and Functional Analyses of the Ministry of Education, Culture, Sports, Science and Technology of Japan. The costs of publication of this article were defrayed in part by the payment of page charges. This article must therefore be hereby marked "*advertisement*" in accordance with 18 U.S.C. Section 1734 solely to indicate this fact.

The atomic coordinates and structure factors (code 2DRE) have been deposited in the Protein Data Bank, Research Collaboratory for Structural Bioinformatics, Rutgers University, New Brunswick, NJ (http://www.rcsb.org/).

[1] Received a scholarship from the Protein Research Foundation in 2005. Present address: Laboratory of Cell Signaling and Metabolism, National Institute of Biomedical Innovation, Ibaraki 567-0085, Japan.

[2] These authors are members of the Structural Biology Sakabe Project (SBSP).

[3] To whom correspondence should be addressed: Dept. of Biomolecular Science, Toho University, Funabashi 274-8510, Japan. Tel./Fax: 81-4-7472-7601; E-mail: auchida@biomol.sci.toho-u.ac.jp.

[4] The abbreviations used are: WSCP, water-soluble chlorophyll-binding protein; Chl, chlorophyll; r.m.s.d., root-mean-square Cα deviation; LHC-II, light-harvesting complex of photosystem II.

WSCP-Chl complex without carotenoids in fact demonstrated that the light-induced singlet oxygen formation of WSCP-bound Chl is four times lower than that of free Chl (1). To clarify what mechanisms other than quenching by carotenoids may protect WSCP-bound Chl against photooxidation, we solved the crystal structure of the native tetrameric WSCP-Chl complex purified from *Lepidium virginicum* (Virginia pepperweed) at 2.0 Å resolution. This is the first report on the crystal structure of a WSCP-Chl complex.

EXPERIMENTAL PROCEDURES

Protein Preparation and Crystallization—WSCP-Chl complex was prepared from the leaves of *L. virginicum* cultivated in Chiba, Japan, and purification was performed by a combination of ammonium sulfate precipitation, anion exchange chromatography, detergent-free polyacrylamide gel electrophoresis, and gel filtration chromatography as described in (14–16) with some modifications. The modifications were that the fraction of 40–90% ammonium sulfate precipitation of the homogenate was separated by DE52 DEAE cellulose chromatography (Whatman Plc, Brentford, UK) in which the elution buffer was 0.2 M sodium/potassium phosphate, pH 7.0, and the final gel filtration chromatography with a Sephacryl S-200 HR (GE Healthcare) was performed with 0.1 M sodium/potassium phosphate pH 7.0. The yield of homogeneously purified WSCP-Chl complex was 30 mg/kg leaves. Fractions with $A_{663}/A_{280} > 1.35$ were used for crystallization. The protein concentration was quantified using bicinchonic acid (BCA; Sigma) and adjusted to 12 mg/ml using the Amicon Ultra-15 (Millipore, Billerica, MA). Crystals of WSCP-Chl complex were grown by means of vapor diffusion by mixing 2 μl of a protein solution containing 0.1 M sodium/potassium phosphate, pH 6.0, with 2 μl of a reservoir solution containing 5% sucrose, 3.2 M ammonium sulfate, and 0.1 M sodium/potassium phosphate, pH 6.0, at 20 °C. Green rhombic crystals appeared 1 week later and grew to a maximum size of ~0.3 × 0.3 × 0.3 mm after 3 weeks (2). Two heavy-atom derivatives were prepared by soaking the crystals for 1 day in the same reservoir solution supplemented with 1.0 mM $K_2Pt(CN)_4$ or 1.0 mM $KAu(CN)_2$.

Diffraction Data Collection, Phasing, Model Building, and Refinement—X-ray data of native crystals were collected at the Photon Factory's (Tsukuba, Japan) beamline BL6A at a wavelength of 0.978 Å. The data sets of derivative crystals were collected with an in-house Rigaku R-AXIS IIc imaging plate system mounted on a Rigaku rotating anode generator at a wavelength of 1.54 Å. Crystals were mounted in a fiber loop and flash-frozen, without any additional cryoprotectant, in a cold nitrogen stream for x-ray data collection. All data were collected at 100 K. The HKL-2000 program package (17) was used for data reduction and analysis. The crystallographic statistics are listed in Table 1. The WSCP-Chl complex crystallized in space group $P2_12_12_1$ with one tetramer per asymmetric unit (Matthews coefficient: 2.2 Å^3/Da). The structure was solved with the multiple isomorphous replacement method using two derivative crystals and the programs MLPHARE in CCP4 (18) and SHARP (19). Model building was performed with the program O (20) and refined with the program CNS (21) without the use of non-crystallographic symmetry restraints. The position of the central Mg^{2+} ion of each Chl molecule was manually refined, without stereochemical restraints between the carbonyl oxygen of Pro36 and the Mg^{2+} ion, by inspecting the σ_A-weighted $F_o - F_c$ omit map with a contour level of 4.0 σ. The final model contained 699 of 720 residues, 4 Chl molecules, and 555 water molecules. Based on the σ_A-weighted $2F_o - F_c$ omit map, all of the four Chl molecules in the asymmetric unit were assigned as Chl-*a* molecules. The model was then checked with the programs PROCHECK (22) and WHAT-CHECK (23). The root mean square deviations of Cα atoms were calculated with the program LSQKAB in CCP4 (18), the volume of the Chl-binding cavity with the program VOIDOO (24), and the water-accessible surface area and buried molecular surface area with the program SurfRace (25).

RESULTS

Characterization, Crystallization, and Structure Determination—The absorption spectrum of the purified complex with a peak wavelength of the red absorption band at 663 nm is identical to that previously reported for CP633 (14, 26). The molecular weight of the WSCP monomer was 19,611 Da as measured by matrix-assisted laser desorption ionization time-of-flight mass spectrometry. Each monomer has the same amino acid sequence deduced from its cDNA (UniProtKB/TrEMBL entry O04797) with the deletion of 26 N-terminal and 17 C-terminal residues. The processing at both terminals of each chain produces the primary structure of the mature WSCP 180 residues. Similar processing of mature WSCPs from Brassicaceae has been reported previously (2, 5, 15). The structure was determined at 2.0 Å resolution with the multiple isomorphous replacement method using platinum and gold derivatives (Fig. 1*a* and Table 1).

Overall Structure of the Homo-tetrameric WSCP-Chl Complex—The oligomeric state is a homotetramer structure, which is consistent with the gel filtration data (80 kDa) (14). There are four Chl molecules at the center of the tetramer, each of which binds stoichiometrically to a monomer of WSCP. The resolved atomic model is of high quality around the Chl-binding region, but both the N- and C-terminals and some outer loops are disordered. The following residues of chain A (1, 163–168, 180), chain B (1–3, 139–141, 180), and chains C, D (1, 2, 180) are disordered and their electron density is too weak for model building.

Each protein chain shows a typical β-trefoil fold comprised of twelve β-strands, of which strands 1, 4, 5, 8, 9, and 12 form a β-barrel that is covered by three two-stranded antiparallel β-sheets composed of the remaining six strands (Fig. 1*b*). This protein folding is often found in Künitz-type serine protease inhibitors. For example, the Dali server identified the trypsin inhibitor from *Delonix regia* seeds (DrTI) (Protein Data Bank ID: 1R8N (27)), whose primary structure is 32% identical with that of WSCP, as being capable of superimposition on chain A of the WSCP tetramer with a root-mean-square Cα deviation (r.m.s.d.) of 2.2 Å (Z-score: 21.1) (28). Although the possibility of the physiological function of WSCP as a proteinase inhibitor has been discussed before, no significant inhibition has thus far been detected (4–6).

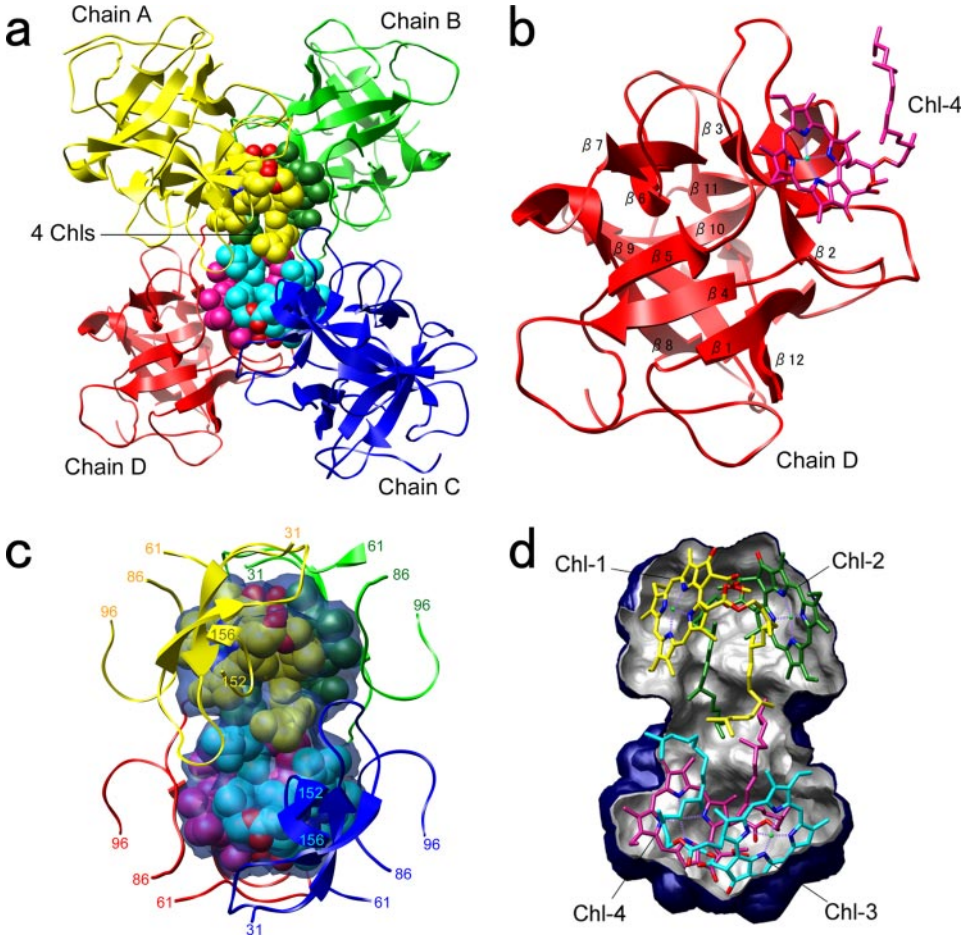

FIGURE 1. **Overall structure of the tetrameric WSCP-Chl complex and Chl-binding cavity.** *a*, the overall structure is shown in a ribbon model of the protein moiety (WSCP) and in a Corey-Pauling-Koltun model of Chl molecules. The four monomers are shown in *yellow*, *green*, *blue*, and *red*. The principal dimers are the pairs of chains A and B and chains C and D. *b*, chain D of the tetrameric WSCP-Chl complex (*ribbon model*) and Chl-4 (*stick model*) are shown with the same orientation as in *a*. *c*, the hydrophobic cavity enclosing the four Chl molecules is shown as a *blue transparent surface*. The residues of 31–61, 86–96, and 152–156 of each WSCP monomer are shown. *d*, a cut-away view of the surface of the cavity shown in *dark blue* (outside) and *silver* (inside). The four Chl molecules are shown in a *stick model* with the same color coding as in *a*. Molecular graphics were generated with the program Chimera (41).

Tetrameric Assembly of the WSCP-Chl Complex and Formation of the Chl-binding Cavity—The four chains that constitute the tetramer can be superimposed on one another with an r.m.s.d. of 0.87 Å and are related by a nearly strict 222 symmetry except for the outer loops of the tetramer, which deviate appreciably from this symmetry. The molecular surface areas buried between pairs of monomers are 223 $Å^2$ (A/B), 231 $Å^2$ (C/D), 174 $Å^2$ (A/D), 190 $Å^2$ (B/C), 57 $Å^2$ (A/C), and 59 $Å^2$ (B/D). The WSCP tetramer can, therefore, be described as a dimer of dimers, where the combinations of chains A and B, and C and D, are the principal dimers.

At the center of the tetramer, one hydrophobic cavity is formed by the residues 31–61, 86–96, and 152–156 of each chain, in which the four Chl molecules are enclosed (Fig. 1*c*). These residues of the four chains interlock to form the Chl-binding cavity and are superimposed on one another with an r.m.s.d. of 0.26 Å and an almost exact 222 symmetry, indicating that the four chains adopt the same conformation to bind the four Chl molecules. The internal volume of the Chl-binding cavity is 5300 A^3, which is approximately equal to the excluded volume of the four clustered Chl molecules, indicating that the Chl molecules are tightly packed in the cavity and that there is no space in the cavity for bulk solvent (Fig. 1, *c* and *d*). However, one water molecule per Chl is present in the cavity (Fig. 2). Each of the four water molecules forms two hydrogen bonds: one with the keto group at C-13^1 of the Chl plane with a mean distance of 2.72 Å and the other with the epsilon oxygen of the Gln-57 residue that originates from the other chain of the principal dimer, with a mean distance of 2.58 Å. The relatively short distances of these hydrogen bonds may be due to the tight packing of the cavity. The water molecules are inside the cavity and separated from the bulk solvent region by the Gln-57 residue of each chain.

The central Mg^{2+} ion of each Chl molecule has a pentacoordinated structure with a single axial ligand provided by the backbone carbonyl of Pro36 (Fig. 2). This coordination bond length is 2.1 Å, and the central Mg^{2+} ion is displaced by a distance of 0.45 Å from the center of the Chl plane toward the axial ligand. This coordination bond is essential for WSCP binding of Chl, since removal of the central Mg^{2+} ion leads to failure in the Chl binding (1).

Two aromatic amino acid residues, Trp-90 and Trp-154, contact the Chl plane at C-7 (4.2 Å distance) and at C-18 (3.8 Å distance) (Figs. 2 and 3*b*). They are within the range of van der Waals interactions, and consequently they may produce fluorescence quenching of excited Chl by means of electron exchange (29).

Although the Chl cluster is almost completely enclosed within the cavity, there are four pores through which bulk solvent could flow into the cavity (Fig. 3*a*). However, the Chl cluster occludes all four of these pores from the inside, so that influx of bulk solvent into the cavity is impossible. The bulk solvent accessible surface area of the Chl molecules is limited to the ester bond that links the Chl plane with the phytyl tail (Fig. 3*b*). The average accessible surface area of the four Chl molecules is ~7 $Å^2$, which is less than one percent of the molecular surface of a Chl molecule.

Geometry of Chl Molecules in the Chl-binding Cavity—The four Chl molecules in the cavity are related by the pseudo 222 symmetry, which comprises two Chl dimers, Chl-1/Chl-2 and Chl-3/Chl-4 (Figs. 1*d* and Fig. 4). Although the phytyl tail of each Chl molecule disrupts the local 222 symmetry, each Chl

TABLE 1
Crystallographic data and refinement statistics

Data collection statistics[a]			
Data set	Native	$K_2Pt(CN)_4$	$KAu(CN)_2$
Space group	$P2_12_12_1$	$P2_12_12_1$	$P2_12_12_1$
Unit cell (*a*, *b*, *c*) (Å)	73.1, 82.7, 121.9	73.1, 82.8, 121.8	73.2, 82.6, 122.3
Resolution (Å)	28.99–2.00 (2.11–2.00)	82.77–2.50 (2.58–2.50)	68.44–2.00 (2.06–2.00)
R_{merge}[b]	0.068 (0.533)	0.086 (0.316)	0.091 (0.356)
Completeness (%)	99.4 (99.0)	91.3 (82.3)	89.9 (77.9)
$\langle I\rangle/\sigma(I)$	9.1 (1.6)	12.1 (3.1)	12.9 (2.7)
Number of sites		2	4
Phasing power (centric/acentric)[c]		0.76/0.99	0.92/1.08
Mean figure of merit (multiple isomorphous replacement/ after density modification)[d]		0.37/0.82	
Refinement statistics			
Number of reflections	47,901		
R_{work}/R_{free} (%)[e]	24.3/28.0		
Number of atoms (protein/Chl/water)	5353/260/555		
Average *B*-factors (Å^2) (protein/Chl/water)	43.2/33.2/46.7		
r.m.s.d. values from ideal			
Bond length (Å)	0.009		
Angles (°)	1.70		
Ramachandran plot			
Most favored (%)	84.4		
Additionally allowed (%)	14.4		
Generously allowed (%)	1.2		

[a] Values in parentheses are for the highest resolution shell.
[b] $R_{merge} = \sum|I-\langle I\rangle|/\sum I$, where *I* is the integrated intensity of a given reflection.
[c] Phasing power = r.m.s. ($|F_H|/E$); $|F_H|$ is the heavy atom structure amplitude, and *E* is the residual lack of closure.
[d] Figure of merit = $|F(hkl)_{best}|/|F(hkl)|$; $|F(hkl)|$ is the amplitude of an individual structure factor amplitude, and $|F(hkl)_{best}|$ is the best estimate for this amplitude.
[e] $R_{work} = \sum||F_{obs}| - |F_{calc}||/\sum|F_{obs}|$. R_{free} was calculated using 5% of data excluded from refinement.

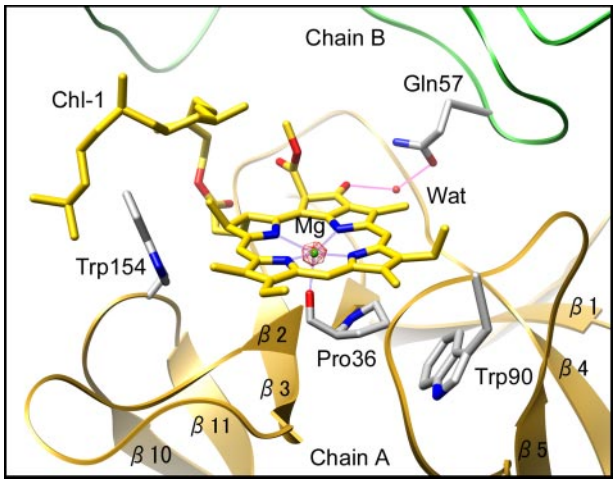

FIGURE 2. **Stoichiometric binding between the WSCP monomer and Chl.** Chains A and B of the WSCP tetramer and Chl-1 are shown in *ribbon models* and a *stick model*, respectively, with the same color coding as in Fig. 1. The σ_A-weighted $2F_o - F_c$ electron density map (4.0 σ contour) for the central Mg^{2+} ion is shown in *pink mesh*. The water molecule in the Chl-binding cavity forms two hydrogen bonds (*pink lines*). Chl-2 is omitted for clarity.

plane almost completely follows the symmetry. The Chl dimer has an "open sandwich" structure, with the Chl planes inclined with respect to the pseudo 2-fold axis. The interplanar angle of the Chl dimer is ~27°. The face-to-face distances between the planes of the Chl dimer are 5.7 Å at the "closed" end (oxygen of the keto group at C-13^1), 9.0 Å at the center (pyrrole nitrogen at N-24), and 10.7 Å at the "open" end (carbon of the methyl group at C-2). The shortest distance between the bulky carboxymethyl groups of the Chl dimer is 3.6 Å. The strength of dipole-dipole coupling V (cm^{-1}) of the Chl dimer was calculated to be 96 cm^{-1} by using the equation $V = 90\kappa/R^3$, where the orientation factor $\kappa = 1.07$ and the center distance $r = 1.0$ nm were determined by the geometry of the Chl dimer, and the proportionality constant was set on the basis of two assumptions, namely, that the value of the refractive index of the immediate environment of chlorophyll is 1.55, and the Chl dimer comprises two Chl-*a* molecules (30). The close proximity of the Chl planes and the estimated *V* value of almost 100 cm^{-1} indicate that the Chl dimer could be regarded as a supermolecule with delocalized electronic transitions, that is, an exciton-coupled dimer.

In the Chl dimer, the two Chl planes sandwich their own phytyl tails, which protrude at the open end (Figs. 1*d* and 4). There are two Chl dimers in the Chl-binding cavity, with their open ends facing each other. Consequently, the four phytyl tails of the Chl molecules generate a hydrophobic interaction at the center of the cavity. Because it has been reported that the phytyl tail of Chl is essential for the oligomerization of the WSCP-Chl complex (1), the hydrophobic interaction among the phytyl tails can be assumed to be the main contributor to the tetrameric assembly of the WSCP-Chl complex.

The Chl-a/b Ratio in the WSCP-Chl Complex—A previous study has demonstrated that the WSCP tetramer isolated from *L. virginicum* has a Chl-*a*/*b* ratio of ~2 (14). In our crystallographic study, this Chl-*a*/*b* ratio was examined by means of the electron density maps. Chl-*b* is identical to Chl-*a* except at the C-7 position, where a formyl group (Chl-*b*) replaces the methyl group (Chl-*a*). When Chl-*b* was assigned to the present structure of the WSCP-Chl complex, negative electron density (σ_A-weighted $F_o - F_c$ map with a contour level of $-3.0\ \sigma$) appeared around the formyl oxygen, but it disappeared when the occupancy of the formyl oxygen was reduced to less than 0.33. In addition, the formyl oxygen was able to form a hydrogen bond with the nitrogen of Leu-91 at a distance of 3.0 Å and without steric hindrance. These results indicate that Chl-*b* may also bind to WSCP in a manner similar to that of Chl-*a*. However, because the σ_A-weighted $2F_o - F_c$ omit map around the formyl oxygen was ambiguous, all four of the Chl molecules were

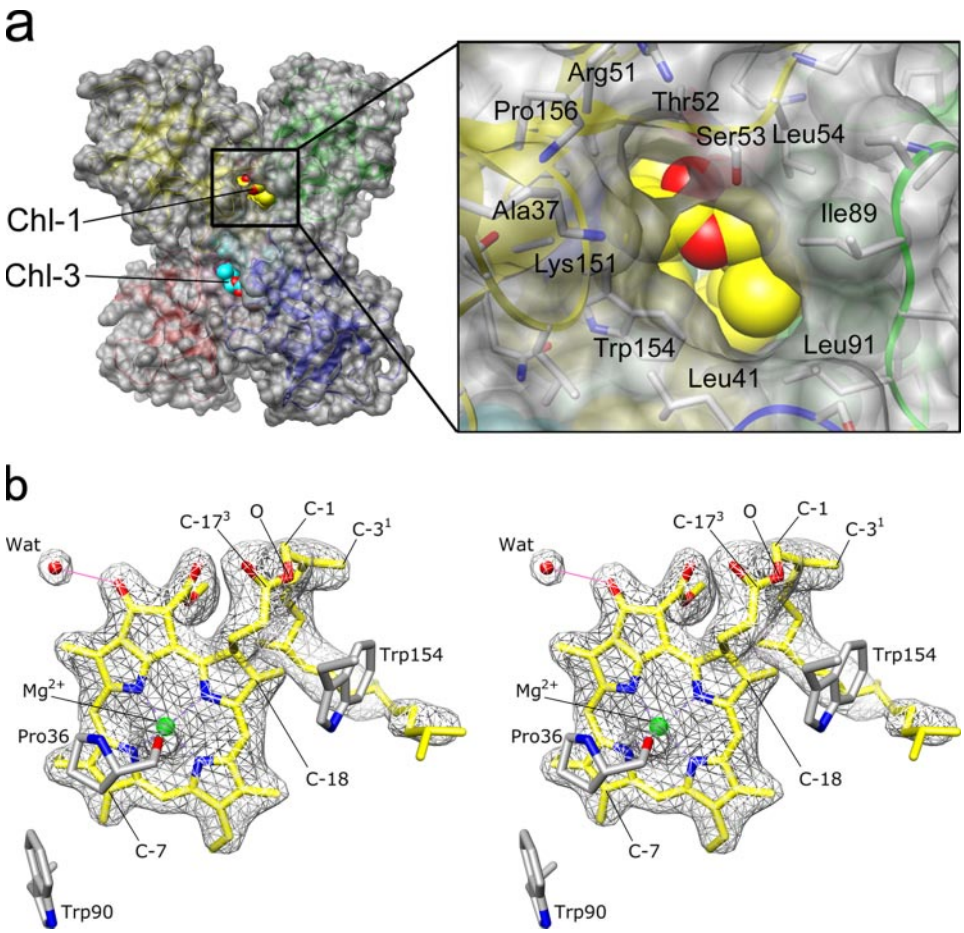

FIGURE 3. **Solvent-accessible part of the Chl molecules in the cavity.** *a*, the tetrameric WSCP-Chl complex is shown with the same orientation as in Fig. 1*a* with the protein surface shown in *transparent gray*. The ester bond region of Chl-1 (*yellow*) and of Chl-3 (*cyan*) shown in the CPK model occlude the pores of the Chl-binding cavity from inside. The other two pores on the flipside of the WSCP tetramer are occluded by Chl-2 and Chl-4 in the same way (data not shown). The *inset* is a close-up view of the pore facing Chl-1. The protein residues forming the edge of the pore are labeled. Since the Chl molecules are enclosed by the protein moiety, bulk solvent access to the Chl molecules is limited. *b*, stereo diagram of the final σ_A-weighted $2F_o - F_c$ electron density map for Chl-1 with a contour level of 1.5 σ. The carbonyl oxygen of Pro-36 is coordinated to the central Mg^{2+} ion of Chl-1. The water molecule forming the hydrogen bond in the cavity is shown as a *red sphere*. The bulk solvent-accessible atoms of Chl-1 (C-17^3, O, C-1, C-3^1) are labeled with IUPAC nomenclature. The carbon atoms of C-7 and C-18 are contacted by Trp-90 and Trp-154, respectively.

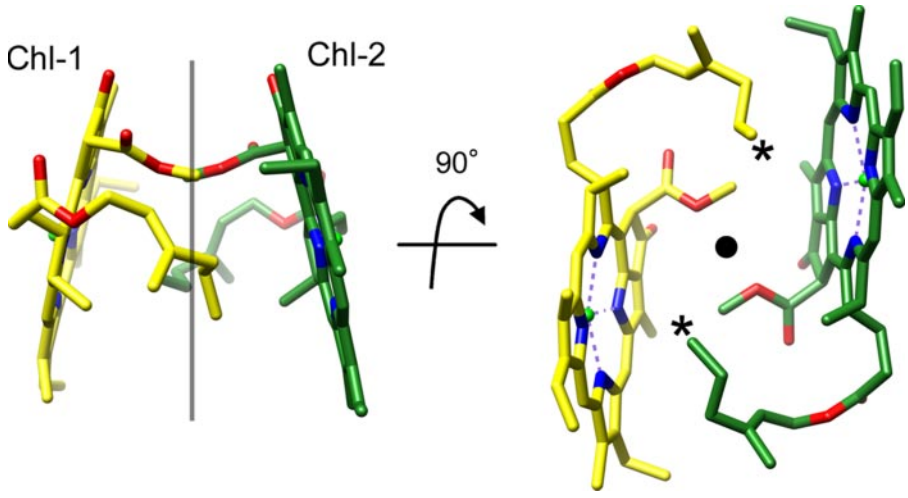

FIGURE 4. **Geometry of the Chl-1/Chl-2 dimer in the tetrameric WSCP-Chl complex.** Views are orthogonal (*left*) and parallel (*right*) to the pseudo 2-fold axis of the Chl dimer. The *black line* (*left*) and the *black circle* (*right*) represent the pseudo 2-fold axis. The *right view* is from the open end of the dimer. The phytyl tails have been truncated (*) for clarity.

reevaluated in the final refined model and were determined to be Chl-*a* molecules.

DISCUSSION

Role of Chl in WSCP Architecture—In this study, we solved the crystal structure of the tetrameric WSCP-Chl complex that comprises four monomers of this soluble protein and four Chl molecules. It has a distinct structure that enables the transportation of the extremely hydrophobic Chl in an aqueous environment. There is a manifest difference between the structural role of Chl in the WSCP-Chl complex and in the membrane-integrated protein-Chl complexes, such as the light-harvesting complex of photosystem II (LHC-II) (31) and photosystem-I (32). The protein architecture of photosynthetic apparatuses largely depends on the presence of Chl molecules intercalated in the membrane-spanning helices. In the WSCP complex, the Chl molecule is attached to the molecular surface of the protein monomer, indicating that its contribution to protein folding of WSCP is minor.

Chl-binding Mode of WSCP—Chl binding of WSCP depends entirely on the coordination bond between the carbonyl oxygen of Pro-36 and the central Mg^{2+} ion of Chl, since pheophytin, a Chl derivative lacking the central Mg^{2+} ion, cannot bind to WSCP (1). The unambiguous electron density of the coordination bond and its bond length of 2.1 Å indicate that the bond is sufficiently strong to maintain the binding of Chl (Figs. 2 and 3*b*).

Chl molecules in LHC-II are bound by the protein matrix from the *anti*-side more frequently than from the *syn* side at a ratio of 11:3. *Syn* and *anti* denote the orientation of the magnesium ligand with respect to the 17-propionic acid esterified by the phytyl tail. The same tendency has also been observed in photosystem-I (33) and other bacteriochlorophyll proteins (34). On the other hand, the axial ligand of Chl in WSCP (Pro-36)

resides at the *syn* side. It has been reported that apo-WSCP can remove Chl from the thylakoid membrane *in vitro*, but the molecular mechanism is not yet understood. It is conceivable that the reason for this unusual Chl-binding mode is that apo-WSCP (Pro36) can form the coordination bond needed to remove Chl directly from the photosynthetic apparatuses by approaching from the *syn* side opposite the protein matrix of LHC-II resides.

We also found that the WSCP monomer stoichiometrically binds one Chl in the tetrameric WSCP-Chl complex. The hydrophobic Chl-binding cavity is formed among the interfaces of all four monomers at the center of the tetramer, where all four Chl molecules are tightly packed. At the same time, hydrophobic interaction among the four phytyl tails is generated in the cavity, which can be considered to be the driving force of WSCP tetramerization. In fact, no oligomerization occurs when the WSCP monomer binds chlorophyllide, which is a Chl derivative lacking the phytyl tail (1).

Possible Mechanisms of Photoprotective Function—The Chl-binding cavity is not completely closed, since there are four pore-like vents in the cavity wall. However, solvent influx through these vents can be ruled out, because the Chl cluster occludes them from inside the cavity. The bulk solvent-accessible surface area of the Chl molecules is limited to the ester bond that links the Chl plane and the phytyl tail. It is generally believed that the generation of singlet oxygen occurs by direct contact, especially with the central Mg^{2+} ion of Chl (35). We therefore propose that the photoprotection mechanism of the WSCP-Chl complex would depend on the tetrameric assembly that encloses Chl molecules in a watertight cavity, since the enclosure reduces the chance of direct contact between the Chl molecules and molecular oxygen.

A question then arises as to how the light-induced excitation energy of Chl is dissipated in the hydrophobic cavity of WSCP. It has been reported that the Chl molecules in the WSCP complex emit fluorescence (3, 26), indicating that the excitation energy of Chl is at least partly dissipated by the fluorescence emission. In addition, the structure solved herein suggests two other possibilities. One is that the excitation energy quenching may be caused by a sequence of electron exchanges between the Chl molecules and the nearby aromatic residues, Trp-90 and Trp-154. Such a quenching mechanism of a light-excited chromophore has been well demonstrated in riboflavin-binding proteins, in which electron exchange efficiently occurs with two nearby aromatic residues (Tyr-75 and Trp-156) that sandwich riboflavin in a hydrophobic cleft (36). The possible involvement of aromatic residues in fluorescence quenching of bacteriochlorophyll and Chl molecules is also discussed in (29, 37, 38).

The other possibility is that the close proximity of the two Chl molecules in the Chl dimer that is formed in the tetrameric WSCP-Chl complex may cause the fluorescence quenching, thereby leading to energy dissipation. It has been suggested that Chl dimers may have the potential to be a powerful quencher, since the one formed in Chl solution exhibits fluorescence quenching *in vitro* (39). Although the mechanism remains to be clarified, it has been proposed that the fluorescence quenching leading to energy dissipation may be caused by energy transfer between Chl molecules. In the Chl-binding cavity of the WSCP-Chl complex, the two Chl molecules of the Chl dimer are related by the nearly exact 2-fold symmetry, where they form the open sandwiched structure at a distance of 10 Å between the centers of the Chl planes (Fig. 4). The geometrically estimated dipole-dipole coupling strength of 96 cm^{-1} indicates that the two Chl molecules could be considered to constitute an exciton-coupling dimer, which allows for energy transfer between them. These results are in accordance with the findings of spectroscopic studies on circular dichroism (1) and magnetic circular dichroism (40). It is therefore an intriguing hypothesis that energy transfer between the Chl molecules may contribute to the photoprotection of Chl molecules in WSCP.

Acknowledgments—We thank Dr. M. Suzuki, Dr. H. Yamamoto, Dr. S. M. Daron, Dr. S. Ohsima, Dr. K. Nakayama, and Dr. M. Okada for their helpful comments; the undergraduate students of the Department of Biomolecular Science of Toho University for sharing their unpublished data; Dr. T. Tsukihara for advice on the phase determination; and the staff of beamline BL6A of the Photon Factory for assistance with the data collection.

REFERENCES

1. Schmidt, K., Fufezan, C., Krieger-Liszkay, A., Satoh, H., and Paulsen, H. (2003) *Biochemistry* **42,** 7427–7433
2. Satoh, H., Uchida, A., Nakayama, K., and Okada, M. (2001) *Plant Cell Physiol.* **42,** 906–911
3. Satoh, H., Nakayama, K., and Okada, M. (1998) *J. Biol. Chem.* **273,** 30568–30575
4. Nishio, N., and Satoh, H. (1997) *Plant Physiol.* **115,** 841–846
5. Ilami, G., Nespoulous, C., Huet, J. C., Vartanian, N., and Pernollet, J. C. (1997) *Phytochemistry* **45,** 1–8
6. Kamimura, Y., Mori, T., Yamasaki, T., and Katoh, S. (1997) *Plant Cell Physiol.* **38,** 133–138
7. Takamiya, K., Tsuchiya, T., and Ohta, H. (2000) *Trends Plant Sci.* **5,** 426–431
8. Hörtensteiner, S. (1999) *Cell. Mol. Life Sci.* **56,** 330–347
9. Matile, P., Schellenberg, M., and Vicentini, F. (1997) *Planta* **201,** 96–99
10. Spikes, J. D., and Bommer, J. C. (1991) in *Chlorophylls* (Scheer., H., eds) pp. 1181–1204, CRC Press, Boca Raton, FL
11. Krieger-Liszkay, A. (2005) *J. Exp. Bot.* **56,** 337–346
12. Niyogi, K. K., Grossman, A. R., and Bjorkman, O. (1998) *Plant Cell* **10,** 1121–1134
13. Szabó, I., Bergantino, E., and Giacometti, G. M. (2005) *EMBO Rep.* **6,** 629–634
14. Murata, T., and Ishikawa, C. (1981) *Biochim. Biophys. Acta* **635,** 341–347
15. Horigome, D., Satoh, H., and Uchida, A. (2003) *Acta Crystallogr. Sect. D Biol. Crystallogr.* **59,** 2283–2285
16. Murata, T., Itoh, R., and Yakushiji, E. (1980) *Biochim. Biophys. Acta* **593,** 167–170
17. Otwinowski, Z., and Minor, W. (1997) *Methods Enzymol.* **276,** 307–326
18. Collaborative Computational Project No. 4 (CCP4) (1994) *Acta Crystallogr. Sect. D Biol. Crystallogr.* **50,** 760–763
19. de la Fortelle, E., and Bricogne, G. (1997) *Methods Enzymol.* **276,** 472–494
20. Jones, T. A., Zou, J. Y., Cowan, S. W., and Kjeldgaard, M. (1991) *Acta Crystallogr. Sect. A* **47,** 110–119
21. Brünger, A. T., Adams, P. D., Clore, G. M., DeLano, W. L., Gros, P., Grosse-Kunstleve, R. W., Jiang, J. S., Kuszewski, J., Nilges, M., Pannu, N. S., Read, R. J., Rice, L. M., Simonson, T., and Warren, G. L. (1998) *Acta Crystallogr. Sect. D Biol. Crystallogr.* **54,** 905–921
22. Laskowski, R. A., MacArthur, M. W., Moss, D. S., and Thornton, J. M. (1993) *J. Appl. Crystallogr.* **26,** 283–291

23. Hooft, R. W., Vriend, G., Sander, C., and Abola, E. E. (1996) *Nature* **381,** 272
24. Kleywegt, G. J., and Jones, T. A. (1994) *Acta Crystallogr. Sect. D. Biol. Crystallogr.* **50,** 178–185
25. Tsodikov, O. V., Record, M. T., Jr., and Sergeev, Y. V. (2002) *J. Compt. Chem.* **23,** 600–609
26. Sugiyama, K., and Murata, N. (1978) *Biochim. Biophys. Acta* **503,** 107–119
27. Krauchenco, S., Pando, S. C., Marangoni, S., and Polikarpov, I. (2003) *Biochem. Biophys. Res. Comm.* **312,** 1303–1308
28. Holm, L., and Park, J. (2000) *Bioinformatics* **16,** 566–567
29. Dashdorj, N., Zhang, H., Kim, H., Yan, J., Cramer, W. A., and Savikhin, S. (2005) *Biophys. J.* **88,** 4178–4187
30. Amerongen, H. V., and Grondelle, R. V. (2001) *J. Phys. Chem. B* **105,** 604–617
31. Liu, Z., Yan, H., Wang, K., Kuang, T., Zhang, J., Gui, L., An, X., and Chang, W. (2004) *Nature* **428,** 287–292
32. Jordan, P., Fromme, P., Witt, H. T., Klukas, O., Saenger, W., and Krauss, N. (2001) *Nature* **411,** 909–917
33. Balaban, T. S., Fromme, P., Holzwarth, A. R., Krauss, N., and Prokhorenko, V. I. (2002) *Biochim. Biophys. Acta* **1556,** 197–207
34. Oba, T., and Tamiaki, H. (2002) *Photosynth. Res.* **74,** 1–10
35. Drzewiecka-Matuszek, A., Skalna, A., Karocki, A., Stochel, G., and Fiedor, L. (2005) *J. Biol. Inorg. Chem.* **10,** 453–462
36. Zhong, D., and Zewail, A. H. (2001) *Proc. Natl. Acad. Sci. U. S. A.* **98,** 11867–11872
37. Li, Y. F., Zhou, W., Blankenship, R. E., and Allen, J. P. (1997) *J. Mol. Biol.* **271,** 456–471
38. Peterman, E. J. G., Wenk, S. O., Pullerits, T., Pålsson, L. O., Grondelle, R. V., Dekker, J. P., Rögner, M., and Amerongen, H. V. (1998) *Biophys. J.* **75,** 389–398
39. Beddard, G. S., and Porter, G. (1976) *Nature* **260,** 366–367
40. Hughes, J. L., Razeghifard, R., Logue, M., Oakley, A., Wydrzynski, T., and Krausz, E. (2006) *J. Am. Chem. Soc.* **128,** 3649–3658
41. Pettersen, E. F., Goddard, T. D., Huang, C. C., Couch, G. S., Grenblatt, D. M., Meng, E. C., and Ferrin, T. E. (2004) *J. Comput. Chem.* **25,** 1605–1612

Structural Mechanism and Photoprotective Function of Water-soluble Chlorophyll-binding Protein

Daisuke Horigome, Hiroyuki Satoh, Nobue Itoh, Katsuyoshi Mitsunaga, Isao Oonishi, Atsushi Nakagawa and Akira Uchida

J. Biol. Chem. 2007, 282:6525-6531.
doi: 10.1074/jbc.M609458200 originally published online December 14, 2006
